IVYSPRING INTERNATIONAL PUBLISHER

Theranostics

2017; 7(15): 3653-3666. doi: 10.7150/thno.18183

Research Paper

Dexamethasone-loaded Polymeric Nanoconstructs for Monitoring and Treating Inflammatory Bowel Disease

Aeju Lee[1,2], Claudia De Mei[1], Miguel Fereira[1], Roberto Marotta[1], Hong Yeol Yoon[3], Kwangmeyung Kim[3], Ick Chan Kwon[3], Paolo Decuzzi [1]✉

1. Laboratory of Nanotechnology for Precision Medicine, Fondazione Istituto Italiano di Tecnologia, Genova, Italy
2. International Research Organization for Advanced Science and Technology (IROAST) and Magnesium Research Center (MRC), Kumamoto University, Japan
3. Center for Theragnosis, Biomedical Research Institute, Korea Institute of Science and Technology, Seoul, Republic of Korea

✉ Corresponding author: Paolo Decuzzi, PhD. Phone: +39 010 71781 941, Fax: +39 010 71781 228, E-mail: Paolo.Decuzzi@iit.it

Received: 2016.11.02; Accepted: 2017.02.20; Published: 2017.08.23

Abstract

Corticosteroids, such as dexamethasone (DEX), are the mainstays for the treatment of moderate to severe inflammatory bowel disease (IBD). However, their relatively poor bioavailability and lack of specificity is often the origin of short and long-term adverse effects. Here, spherical polymeric nanoconstructs (SPNs) encapsulating dexamethasone are proposed for the systemic treatment of IBD. In a mouse model of colitis, the accumulation of SPNs within the inflamed intestine is firstly assessed using near infra-red fluorescent (NIRF) imaging at different stages of the disease – 5, 7 and 10 days of Dextran Sulfate Sodium (DSS) administration. Then, the efficacy of DEX-SPNs is tested in vitro over macrophages and in vivo by monitoring the animal weight, food and water intake; expression of inflammatory cytokines (TNF-α, IL-1β, IL-6); intestinal density of macrophages; rectal bleeding and histological scoring. 150 nm DEX-SPNs are shown to deposit within the hyper-permeable inflamed intestine in a disease severity-dependent fashion. DEX-SPNs exposed to LPS-stimulated RAW 264.7 cells reduce the expression of inflammatory cytokines as rapidly as free DEX. In DSS-administered mice, DEX-SPNs treatments improve weight loss, reduce the macrophage infiltration, expression of inflammatory cytokines, rectal bleeding and histological scoring, as compared to free DEX. Moreover, DEX-SPNs exert a strong systemic anti-inflammatory effect and facilitate animal recovery. This work confirms the benefits of using sufficiently small nanoconstructs for targeting inflamed, hyper-permeable tissues and efficiently delivering high doses of corticosteroids for the treatment of intestinal and systemic inflammation.

Key words: nanoparticles, chronic inflammation, immune cells

Introduction

Inflammatory bowel disease (IBD) is a chronic inflammation of the gastrointestinal tract which is clinically manifested in the forms of ulcerative colitis and Crohn's disease.[1, 2] Ulcerative colitis generally localizes within the rectum and colon and is characterized by a diffuse neutrophil infiltration within the intestinal mucosa, often inducing a profound alteration in the architecture of the mucosal crypts. Differently, Crohn's disease develops along the whole gastrointestinal tract and its histopathological hallmark is the formation of granulomas, resulting from the clustering of macrophages and plasma cells. Although the genetic and environmental origins of the disease are still a matter of intense research and debate[3-5], IBD is associated with extensive migration across the vascular endothelium and deep infiltration within the epithelium of immune cells.[2, 6-8] The accumulation of neutrophils, macrophages, and dendritic cells within the inflamed areas correlates with an overall increase in intestinal permeability to molecules, macromolecules, and cells. The hyper-permeability of

vascular beds and extravascular compartment has been also recognized as an early stage in the development of inflammatory bowel disease.[9-12]

Given the strong inflammatory component, the first line of treatment for IBD involves the use of anti-inflammatory molecules, such as aminosalicylates (5-aminosalicylic acid); followed by corticosteroids (prednisone, hydrocortisone, dexamethasone); monoclonal antibodies, against inflammatory cytokines (anti-TNF-α antibodies) and vascular adhesion molecules (anti-integrin antibodies); and cytotoxic drugs with strong anti-inflammatory effects (methotrexate).[13] While aminosalicylates are used for moderate manifestations of the disease, therapeutic interventions based on the administration of anti-inflammatory molecules, monoclonal antibodies and corticosteroids are usually prescribed for moderate to severe conditions. Although the administration of corticosteroids is generally the most effective medical treatment, their long term use is often associated with significant adverse effects.[14] These include sleep and mood disturbance, dyspepsia, increased risk of infection, nausea and vomiting, thrombosis and poor wound healing, hypertension, hyperglycaemia, fluid retention and weight gain and osteoporosis.[15, 16] Such undesirable effects should be ascribed to the lack of any selectivity for systemically injected corticosteroids, thus it is reasonable to speculate that the specific delivery of these potent drugs to inflamed tissues could alleviate any adverse effects.

The encapsulation of therapeutic agents into nanoparticles – nanomedicines – has already demonstrated in the clinic the ability to improve the bioavailability and therapeutic index of drug molecules by increasing specific drug accumulation at the biological target while reducing off-site effects.[17, 18] Nanomedicines can simultaneously carry multiple and different therapeutic molecules to the diseased site, enabling *de facto* combination therapies.[19, 20] Also, the release of any therapeutic agents can be triggered and modulated by endogenous (pH, oxygen and enzyme concentrations, flow shear stresses) and exogenous stimuli (light, heat and ultrasound), further enhancing target specificity.[21] In addition to drug molecules, nanomedicines can also carry agents to enhance contrast in optical, magnetic resonance and nuclear imaging, enabling the multimodal interrogation of the diseased tissue as well as the accurate follow-up on the therapeutic intervention.[20, 22]

Whilst a plethora of different nanomedicines have been proposed for the treatment and imaging of cancerous and atherosclerotic lesions, only a handful of nanoconstructs have been developed for applications in inflammatory bowel disease.[23, 24] Nanomedicines have been shown to accumulate in solid tumors and atherosclerotic plaques by exploiting the hyper-permeable tumor blood vessels, the discontinuous plaque surface and the infiltration of circulating immune cells.[20, 25, 26] Interestingly, tissue hyper-permeability and neutrophil infiltration are key features also in IBD and could be equally exploited to foster the preferential homing of nanomedicines within the inflamed, intestinal tissue.[14]

Inspired by such similarities and motivated by the enhanced therapeutic potential of nanomedicines over freely administered molecules, Dexamethasone-loaded Spherical Polymeric Nanoconstructs (DEX-SPNs) are here proposed for the treatment of inflammatory bowel disease. DEX-SPNs are synthesized, characterized for their physico-chemical and biological properties, and tested in pre-clinical models of Dextran Sodium Sulfate (DSS) induced colitis.[27] The ability of DEX-SPNs in lodging within the inflamed tissue, assessing the severity of the disease via non-invasive near infrared imaging, and inhibiting both localized and systemic inflammation is demonstrated.

Materials and Methods

Synthesis of Cyanine-5 lipid

15 mg of DSPE-NH_2 was dissolved in 3 mL of dichloromethane (DCM) and 1.5mL of MeOH. 0.98 eq of Cyanine-5 NHS ester were dissolve in 200 ml of dimethylformamide (DMF) and added to the previous solution. A catalytic amount of triethylamine (TEA) was added to the reaction and was left to stir for 16 hours. The intended product was precipitated with cold diethyl ether. The product was washed 3 times with cold diethyl ether getting the final product with a yield of 90%. MS (ESI): m/z – calcd for $C_{71}H_{113}N_3O_{15}PS_2$, 1342,73; found, 1342,75.

Preparation of Cyanine-5 SPNs

Spherical Polymeric Nanoconstructs, tagged with Cyanine-5 (Cy5-SNPs), were prepared by a slightly modified sonication-emulsion technique, already described elsewhere.[28] Briefly, carboxyl-terminated poly(lactic-co-glycolic acid) (PLGA) and 1,2-dipalmitoyl-sn-glycero-3-phosphocholine (DPPC), in a 10:1 ratio, were dissolved in chloroform to obtain a homogeneous solution (oil phase). For the superficial lipid monolayer, two lipids were used, namely 1,2-distearoyl-sn-glycero-3-phosphoethanola-mine-N-[carboxy(polyethylene glycol)-2000 (DSPE-PEG-COO H) and 1,2-Distearoyl-sn-glycero-3-phos-phoethanol- amine conjugated with the fluorophore

Cy5 (DSPE-Cy5), with a molar ratio of 5:1, dissolved in the aqueous phase of 4% ethanol. The ratio between the oil phase and the aqueous phase was 1 to 5. To prepare SPNs, the oil phase was added drop wisely to the aqueous phase under ultrasonication. The obtained emulsion was then placed under magnetic stirring, to facilitate solvent evaporation. SPNs were centrifuged first for 5 min at 1,500 rpm, in order to settle down any possible debris, then the supernatant was centrifuged 3 more times for 20 minutes at 12,000 rpm.

Preparation of DEX-SPNs

For the preparation of DEX-SPNs, the same procedure described above was followed. However, in this case, a known amount of dexmethasone acetate (DEX) was dispersed in the oil phase while the DSPE-Cy5 was removed from the aqueous phase. All ratios were kept fixed during this preparation.

Cy5-SPNs and DEX-SPNs size, stability and morphology characterization

Dynamic light scattering (DLS: Malvern Zetasizer Nano S) and transmission electron microscopy (TEM: FEI, Elios Nanolab 650) were employed to characterize SPN size and morphology. DLS was used to assess the radius of SPNs under hydrated conditions. Cryo-EM and cryo-electron tomography were applied to reconstruct single DEX nanoparticles at high resolution. A solution of DEX SPNs, once applied on glow discharged holey TEM grids, was plunge-frozen in liquid ethane cooled at liquid nitrogen temperature using a FEI Vitrobot Mark IV semi-automated cryo-plunger. CryoEM projection images and single-axis tilt series were recorded in low dose using a FEI Tecnai G2 F20 Schottky field emission gun transmission electron microscope, equipped with automated cryobox and a Gatan Ultrascan 2k x 2k CCD detector. The tilt series were acquired from ± 60° with a tilt angle of 2° at a magnification of 25000 times (pixel size of 4.3 Å) with a total electron dose between 60 and 80 $e^-/(A^2s)$. Cryo electron tomograms were calculated and filtered using Imod 3.8.40. The 3D model has been obtained using Amira software (FEI Visualization Group).

Evaluation of drug loading and encapsulation efficacy in DEX SPNs

To calculate the drug amount inside NPs, samples were lyophilized and dissolved in dimethyl sulfoxide (DMSO). All samples were analyzed by HPLC at 240 nm UV absorbance (Agilent 1260 Infinity, Germany). The drug loading is defined as the weight ratio between the considered drug and the DEX SPNs weight, in percentage. The encapsulation efficiency is defined as the percentage weight ratio between the drug amount inside DEX SPNs at the end of their preparation and the initial amount of the input drug.

Drug release DEX SPNs

To confirm the drug release kinetics, DEX SPNs were poured in a Slide-A-Lyzer MINI dialysis microtube with a molecular cut off of 10 kDa (Thermo Scientific) and dialyzed in 4 L of PBS buffer (pH 7.4), at 37 °C. For each time point, triplicate DEX SPNs were collected and the amount of dexamethasone was characterized by high-performance liquid chromatography (HPLC). The cumulative dexamethasone release was calculated based on a standard curve (1.95-1000 µg/ml).

In vitro internalization

RAW 264.7 murine macrophages were cultured in DMEM High Glucose (4.5g/L D-Glucose) supplemented with 10% fetal bovine serum, 1% penicillin/streptomycin at 37 °C and 5% CO_2 atmosphere. To confirm internalization of Cy5-SPNs in activated or inactivated macrophages, 5×10^4 cells were seeded in 35 mm^2 glass-bottom dishes and incubated at 37 °C for 24 h. Cells were treated with or without lipopolysaccharide (LPS, 100 ng) for 6 h and filled fresh media. After 24 h, cells were incubated with 10 µg/ml Cy5-SPNs for 2 h. After washing, cells were fixed with 4% PFA for 15 min and counterstained with Hoechst 33342 (H3570, Life science, USA). Images were obtained using a confocal microscope (Nikon Eclipse Ti-U, Nikon, Japan).

In vitro gene expression

To evaluate the *in vitro* gene expression, RAW 264.7 cells were seeded in 6-well plates (1×10^6 cell) and incubated with 100 ng of LPS for 24 h. The activated cells were treated with media, free DEX (100 nM), Empty NPs, DEX SPNs in each well for 6 and 24h. After treatment, cells were collected and total RNA was extracted using RNA isolation kit (74134, Quiagen). The reverse transcription was performed using a High Capacity RNA to cDNA kit (Applied Biosystems), according to the manufacturer's instruction. The gene expression of TNF-α, IL-1β, IL-6 and GAPDH (internal control) was confirmed by real-time PCR (ViiA7, QIAGEN) using FAST SYBR® Green master mix (Applied Biosystems). The primer sequences were as follows: TNF- α Forward 5′-GGTGCCTATGTCTCAGCCTCTT-3′, Reverse 5′-GCCATAGAACTGATGAGAGGGAG-3′; IL-1β Forward 5′-TGGACCTTCCAGGATGAGGACA-3′, Reverse 5′-GTTCATCTCGGAGCCTGTAGTG-3′; IL-6

Forward 5′-TACCACTTCACAAGTCGGAGG C-3′, Reverse 5′-CTGCAAGTGCATCATCGTTGTTC -3′; GAPDH Forward 5′-CATCACTGCCACCCAGA AGACTG-3′, Reverse 5′-ATGCCAGTGAGCTTCCC GTTCAG-3′. Themocycler conditions were as follows: 95 °C for 2 min, 40 cycles of 95 °C for 15 sec, 60 °C for 30 sec, with a final extension at 55-95 °C (in 0.5 °C increments) for 10 sec. The expression of TNF-α, IL-1β, and IL-6 was determined using $^{\Delta\Delta}$Ct analysis method.

Flow cytometry analysis

Cells were seeded in 6-well plates at 5×10^5 cells/well and incubated overnight. The following day, cells were treated with LPS (100 ng/ml) for 8h. After washing and adding fresh medium without LPS, cells were cultured for additional 16h. Then, cells were incubated with Cy5-SPNs. In order to measure the uptake of labeled SPNs, cells were collected at different time points (15, 30, 60, 120 and 240 min) and Cy5-positive cells were counted with the BD FACS Aria II Cell Sorter (Becton Dickinson & Co).

In vivo imaging in DSS-induced mouse model of colitis

A colitis model was induced in 8 week old C57B/6J female mice (Charles River) using Dextran Sodium Sulfate (DSS; MP Biomediclas) according to previous research.[27] A total of 18 mice were administered with a 4% DSS solution, added to the drinking water, for 5, 7, and 10 days (6 mice each day, respectively). The 9 controlled mice received clean water for 5, 7, and 10 days (3 mice each day, respectively). Before injection Cy5-SPNs, mice were anaesthetized and fur was removed from the intestinal region. The mice were monitored daily for body weight, food intake, water intake, rectal bleeding, survival and stool consistency. All animal procedures were approved by the Institutional Animal Care and Use Committee in accordance with the Italian Ministry of Health policies.

Therapies in DSS-induced mouse model of colitis

Thirty-two, 8 week old C57B/6J female mice were purchased from Charles River. To assess therapeutic efficacy, 24 mice were administered with a 4% DSS solution, added in their drinking water for 7 days. The 8 controlled mice received clean water for 7 days. At 2 days of DSS administration, mice were randomly divided into three groups (n=8, respectively) receiving intravenous injection of Free DEX (5 mg/kg), Empty NPs, or DEX SPNs every other day, until 16 days, for a total of 6 consecutive treatments. The 8 controlled mice received saline. Before injecting Cy5-SPNs, mice were anaesthetized and fur was removed from the intestinal region. Mice were monitored daily for body weight, food intake, water intake, rectal bleeding, survival and stool consistency. For the histological scoring, colons were embedded in OCT compound. Specimens were sectioned into 6 µm slices and stained using the Hematoxylin and Eosin method. Severity of histological change in the colon was scored using a scale of 0-4, where 0 is for no evidence of inflammation, 1 for low level of inflammation with scattered infiltrating mononuclear cells (1–2 foci), 2 for moderate inflammation with multiple foci, 3 for high level of inflammation with increased vascular density and marked wall thickening, 4 for maximal severity of inflammation with transmural leukocyte infiltration and loss of goblet cells. The severity of histological change was determined as the mean score of the colon. Rectal bleeding and histological scoring were performed following standard methods.[29] All animal procedures were approved by the Institutional Animal Care and Use Committee in accordance with the Italian Ministry of Health policies.

In vivo and *ex vivo* near infrared fluorescence (NIRF) imaging

To assess the SPN biodistribution, Cy5-SPNs were injected systemically in DSS-induced colitis mice. Then whole animal fluorescent imaging was performed using an IVIS Spectrum (Cy5; 646 nm excitation & 662 nm emission band-pass filter, Perkinelmer). At 5, 7, and 10 days after DSS administration, mice were injected via tail vein with Cy5-SPNs (n=6 per each group) and monitored via IVIS Spectrum at 1, 4, 8, and 24h post injection. Finally, at 24h post Cy5-SPN administration, mice were sacrifices, major organs harvested and images ex-vivo for NIRF signals with the IVIS Spectrum. All animal procedures were approved by the Institutional Animal Care and Use Committee in accordance with the Italian Ministry of Health policies.

In vivo and *ex vivo* monitoring of disease severity and therapeutic response.

Normal and Free DEX, Empty SPNs, and DEX SPNs treated mice were intravenously injected with Cy5-SPNs (n = 3/group). Injections occurred after 3 and 6 consecutive treatments. At 1, 4, 8, and 24 h post injection of Cy5-SPNs, mice were anaesthetized and whole body NIRF imaging was performed using an IVIS Spectrum. Finally, at 24h post Cy5-SPN administration, mice were sacrifices, major organs harvested and images ex-vivo for NIRF signals with the IVIS Spectrum. All animal procedures were approved by the Institutional Animal Care and Use

Committee in accordance with the Italian Ministry of Health policies.

Ex vivo colon immunofluorescence staining

Harvested tissues were embedded in OCT compound and sectioned into 6 µm slices. Slides were double immunofluorescence stained with primary mouse anti-CD68 antibody and rabbit anti-TNF-α (1:1000, ab9739, abcam), or anti-IL-1β (1:2000, ab9722, abcam) and anti-IL-6 (1:1000, NB600-1131, Novusbio) antibodies, and goat anti-mouse-TRITC (1:5000, ab6786, abcam). Goat anti-rabbit-Alexa Fluor 488 (1:5000, ab150077, abcam) was used as a secondary antibody. Counterstain was performed with Hoechst 33342 and mounted slide. Slides were observed by confocal microscopy. DAPI was excited with a 405 nm laser, and emission was detected at 408-475 nm band-pass-filter. FITC was excited with a 488 nm laser, and emission was detected at 498-551 nm band-pass filter. TRITC was excited with a 561 nm laser, and emission was detected at 563-612 nm band-pass filter. Cy5 was excited with a 633 nm laser, and emission was detected at 640-690 nm band-pass filter.

Ex vivo gene expression

Colon and liver were harvested. Total RNA was extracted using a lipid tissue RNA isolation kit (74804, Quiagen) and the reverse transcription was performed using a High Capacity RNA to cDNA kit according to the manufacturer's instruction. The primer sequences and thermocycler conditions were the same as for the *in vitro* gene expression, described above.

Western blot

Colon and liver (n= 3 per each group) were homogenized and lysate in RIPA buffer (89900, Thermo Scientific). Total protein was calculated using a BCA assay kit (EMP014500, Euroclone) and analyzed by SDS-PAGE (30 ug/ lane) and transferred to nitrocellulose membrane. Protein band was detected with primary rabbit anti-TNF-α (1:1000), or anti-IL-1β (1:500), and anti-IL-6 (1:500) antibody; and mouse anti-GAPDH (1:2000, 398600, Life technologies) antibodies. Goat anti-mouse HRP and goat anti-rabbit HRP were used as secondary antibody. Membrane was visualized using ECL solution (EMP13200, Euroclone) and developed by automatic image detector (LAS-4000, Fujifilm, Japan).

Statistical analysis

Statistical analyses were performed using One-way ANOVA and Tukey's t test. P values of * < 0.05, ** < 0.01 and *** < 0.001 were considered to be statistically significant. All data are presented as means ± SD.

Results

Synthesis and physico-chemical characterization of DEX-SPNs

Spherical polymeric nanoconstructs (SPNs) were prepared by a sonication-emulsion technique, following protocols already described by the authors.[19] Briefly, an oil phase containing a mixture of polymeric and lipid chains – poly(lactic-co-glycolic acid) (PLGA) and dipalmitoylphosphatidylcholine (DPPC) – was added to an aqueous phase containing a mixture of PEGylated lipid chains – DSPE-PEG-COOH – and fluorophores – DSPE-Cy5. Under sonication this mixture forms an emulsion from which SPNs are eventually extracted. The hydrophobic drug molecule dexamethasone (DEX) is added in the oil phase and encapsulated within the SPN core. The structure of SPNs is shown schematically in **Figure 1A** and includes a hydrophobic PLGA core, a lipid monolayer, therapeutic and fluorescent molecules.

SPNs are uniform in size, as confirmed via Transmission Electron Microscopy (TEM) imaging (**Figure 1B**, **Figure S1.A** and **Movie S1**) and Dynamic Light Scattering (DLS) characterizations (**Figure 1C**). Cy5-SPNs and DEX-SPNs present a hydrodynamic diameter of 139.9 ± 5.0 nm and 162.0 ± 8.2 nm with a poly-dispersity index (PDI) of 0.20 ± 0.03 and 0.23 ± 0.02, respectively. The zeta potential is of -34.00 ± 0.49 mV for Cy5-SPNs and of -39.5 ± 2.31 mV for DEX-SPNs **(Figure 1C)**. This proves that DEX loading into SPNs does not significantly alter the nanoconstruct size. Furthermore, for assessing the colloidal stability, the hydrodynamic diameter of DEX-SPNs is monitored via DLS up to 7 consecutive days, in PBS at 37°C. Both the hydrodynamic diameters and PDI are preserved over time **(Figure 1D)**.

Then, DEX-SPNs are characterized in terms of loading efficiency (LE) and encapsulation efficiency (EE), as described in the Materials and Methods section. DEX-SPNs exhibit a LE of 6.93 ± 1.28% and an encapsulation efficiency EE of 39.60 ± 3.21% **(Figure 2A)**. The release profile for DEX-SPNs is shown in **Figure 2B**, where a quasi-linear release is observed over the first 48h followed by a plateau. Almost 90% of the loaded DEX is released within the first 48h whereas the remaining 10% is released within the following 3 days. The inset documents that only 30% of the loaded drug is released within the first 12h. This data suggests a stable loading of DEX within the polymeric matrix which limits any initial burst release and drug leakage in the circulation.

Anti-inflammatory efficacy of DEX-SPNs on macrophages

Cy5-SPNs are used for internalization studies conducted on RAW 264.7 cells activated and not-activated by LPS stimulation. Representative confocal microscopy images, obtained at 2h post incubation of Cy5-SPNs with cells, are shown in **Figure 2C**. The fluorescent images demonstrate a perinuclear localization of Cy5-SPNs already after 2h, whereas the z-stack analysis confirms the intracellular localization of the polymeric nanoconstructs (Blue: DAPI, Red: Cy5-SPNs). Stimulation of RAW 264.7 cells with LPS does not affect significantly the internalization rates (**Figure S1.B**). It is here important to notice that SPNs have been designed to be rapidly uptaken by immune cells and, equally rapidly, release their payload – DEX – into the cells.

In order to confirm the anti-inflammatory efficacy of DEX-SPNs, the concentration of pro-inflammatory cytokines is also analyzed. Specifically, RAW 264.7 cells are incubated with free dexamethasone (Free DEX), empty nanoconstructs (Empty SPNs), and dexamethasone-loaded nanoconstructs (DEX-SPNs). Results are shown in **Figure 2D** for both not-activated and LPS-activated RAW 264.7 cells, at 6 and 24h post incubation. The administration of Free DEX and DEX-SPNs significantly downregulates the expression of the pro-inflammatory genes TNF-α, IL-1β, and IL-6, as compared to the positive control (LPS-activated cells). This is observed both at 6 and 24h although, as expected, the larger modulation in gene expression is associated with the longer time point. In general, the gene downregulation induced by DEX-SPNs is slightly lower as compared to Free DEX. This is a common pattern for all in vitro experiments where nanomedicines must first enter the cell body and then release their payloads, whereas free molecules are immediately active as soon as they cross the cell membrane. However, as shown in the sequel, this pattern is reversed in vivo due to the improved bioavailability and specific tissue accumulation of nanomedicines as compared to freely administered drug molecules.

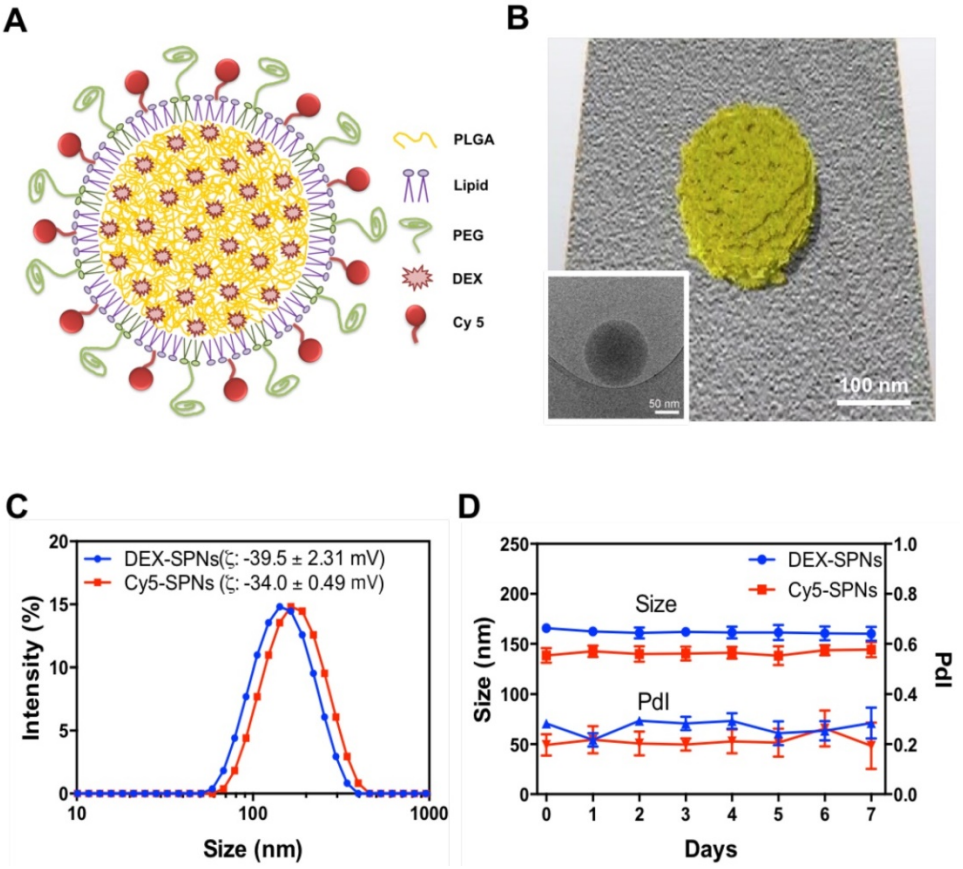

Figure 1. Characterization of Spherical Polymeric Nanoconstructs (SPNs), loaded with dexamethasone (DEX-SPNs) and labeled with a near-infrared dye (Cy5-SPNs). A. Schematic of DEX-SPNs and Cy5-SPNs. B. 3D model and cryo-EM image (inset) of DEX-SPNs in fully hydrated state. C. Size distribution via dynamic light scattering of DEX-SPNs and Cy5-SPNs, at 37 °C in PBS (pH 7.4). D. Temporal stability of DEX-SPNs and Cy5-SPNs, at 37 °C in PBS (pH 7.4). Results are presented as mean ± SD (n=6).

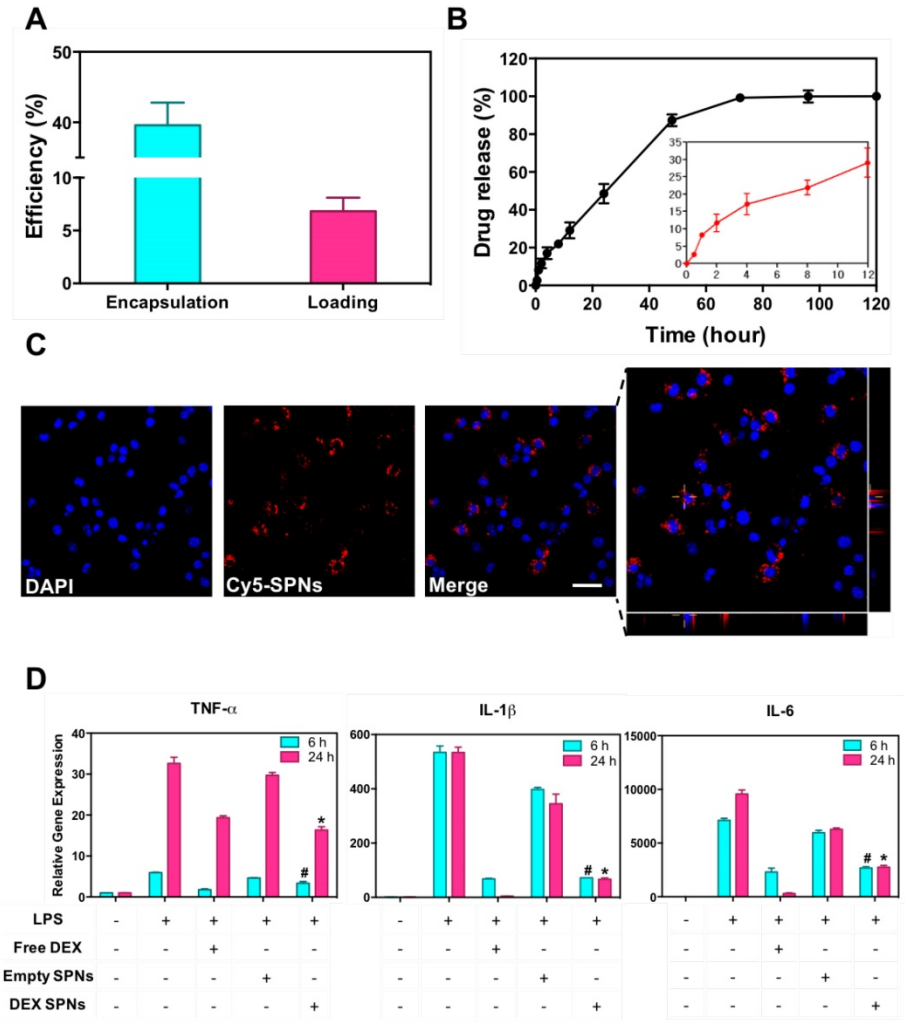

Figure 2. Drug loading and release, and macrophage interaction for DEX-SPNs. A. Dexamethasone encapsulation and loading efficiency in DEX-SPNs. **B.** Dexamethasone release kinetics from DEX-SPNs, at 37 °C in PBS (pH 7.4). **C.** Confocal microscopy analysis of Cy5-SPN internalization in RAW 264.7 cells. (Scale bar: 25 μm) **D.** Relative inflammatory cytokine (TNF-α, IL-1β, and IL-6) gene expression from RAW 264.7 cells following incubation with media (LPS+/-), Free DEX, Empty SPNs, and DEX-SPNs, respectively. Results are presented as mean ± SD (n=6). ([TNF-a: #, p<0.001, 6h, DEX SPNs vs LPS+, Free DEX, Empty SPNs; *, p<0.001, 24h, DEX SPNs vs LPS+, Free DEX, Empty SPNs], [IL-1b: #, p<0.001, 6h, DEX SPNs vs LPS+, Empty SPNs; *, p<0.001, 24h, DEX SPNs vs LPS+, Free DEX, Empty SPNs], [IL-6: #, p<0.001, 6h, DEX SPNs vs LPS+, Empty SPNs; *, p<0.001, 24h, DEX SPNs vs LPS+, Free DEX, Empty SPNs])

Specific tissue accumulation of Cy5-SPNs in a DSS-induced colitis model

A pre-clinical model of inflammatory bowel disease is established by administering a solution of dextran sodium sulfate (DSS) to mice. The severity of the disease is modulated by changing the duration of DSS administration, namely 5, 7 and 10 days. At the end of this period, mice are taken back to normal water.

The accumulation of systemically injected Cy5-SPNs within the inflamed intestinal area is assessed in vivo and ex vivo by using whole animal, near infra-red fluorescent (NIRF) imaging at 24h post nanoconstruct injection. Cy5-SPNs are tail vein injected at day 1 post completion of DSS administration. NIRF imaging of the abdominal area demonstrates the accumulation of Cy5-SPNs within the intestine (**Figure 3A** and **3B**). In healthy mice (control), no signal is observed. In mice administered with DSS, both the intensity and the spatial distribution of the NIRF signal increases significantly as compared to control animals. Specifically, the NIRF signal intensity in mice administered for 5, 7 and 10 days with DSS is about 2, 6, and 8-fold higher than in control animals (**Figure 3B**). This data demonstrates that Cy5-SPNs accumulation within the inflamed tissue is specific and dependent on the disease severity. This is also evident in the NIRF images of the harvested colons (**Figure 3C** and **Figure S2.A**). Cy5-SPNs are mostly confined within the cecum for moderate disease states (≤ 5 days of DSS administration), whereas Cy5-SPNs spread along the whole colon, from proximal to distal, for sever disease states (≥ 5 days administration of DSS). Also, as expected, the length of the colon is observed to reduce

with the disease severity from about 3.2 cm (control) to 2.5 cm (10 days of DSS administration). Finally, H&E staining of the colon **(Figure S2.B)** demonstrates severe erosion, crypt destruction, infiltration of leukocytes and wall thickening proportionate to the disease severity, in agreement with the literature.[27]

During the whole experimental period (35 days), the mouse weight, water and food intakes are monitored on a daily base, as reported in **Figure 3D** and **Figure S2.C-D**. Healthy mice grow continuously in weight, up to about 20% of the original value, in 35 days. Differently, mice administered with DSS significantly reduce their weights and progressively tend to recover only after treatment completion: the longer is the period of DSS administration, the larger is the weight loss and the longer is the recovery period (**Figure 3D**). For a 10 day DSS administration, mice loose up to 20% of their body weight within the first 11 days, present a stable body weight for a week, and progressively reach the body weight of control animals within the following 17 days. On the other hand, for a 5 day DSS administration, mice loose up to 10% of their body weight within the first 7 days and reach the body weight of control animals within the following 5 days. For a 7 day DSS administration, a similar pattern is observed with characteristic values which are intermediate between the 5 and 10 day DSS-administration cases. The water and food intakes **(Figure S2.C-D)** significantly change both during and post DSS administration. In particular, mice treated for 10 days with DSS present a lower water and food intake during the DSS administration followed by a significant increase in water uptake.

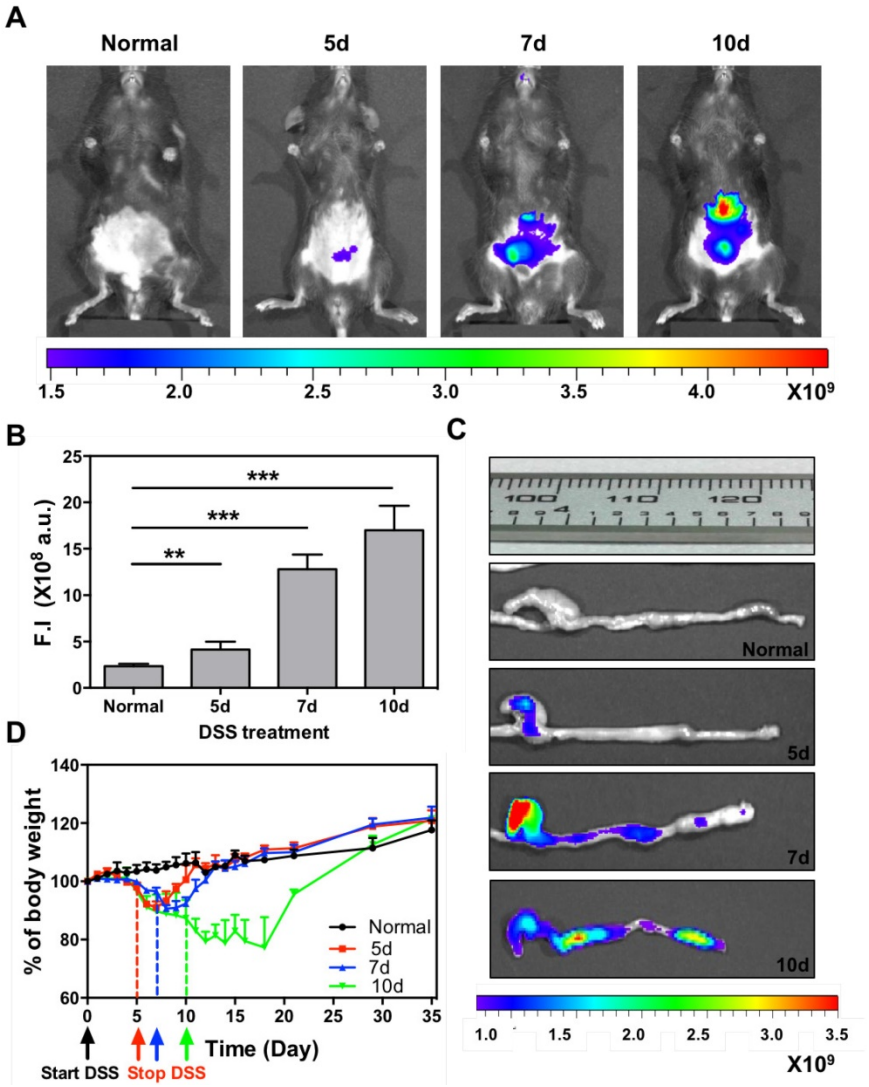

Figure 3. Cy5-SPNs accumulation within the intestine of DSS-induced mouse models of colitis. A. Representative near-infrared fluorescent (NIRF) *in vivo* image of Cy5-SPNs accumulating within the abdominal area in mice administered with DSS for 5, 7 and 10 days. 6 mg of PLGA based Cy5-SPNs were *i.v* injected. **B.** Normalized NIRF signal intensities from the *in vivo* images. **C.** *Ex vivo* colon NIRF imaging and length. **D.** Body weight variation over time of mice administered with DSS. Results are presented as mean ± SD (n=5/group). * $P < 0.05$; ** $P < 0.01$; *** $P < 0.001$

Therapeutic efficacy of DEX-SPNs in a DSS-induced colitis model

For all in vivo therapeutic studies, a 7 day DSS-administration period is considered. At day 2 post initiation of DSS administration, DEX-SPNs are injected systemically every two days, until day 12. This corresponds to a total of 6 injections of 5 mg/kg of DEX equivalent dose. Four experimental groups are considered, namely normal mice (no DSS administration), Empty SPNs, free dexamethasone (Free DEX), and DEX-SPNs. Seven different approaches are used to assess animal response to treatment, namely in vivo and ex vivo NIRF imaging of the abdominal area and colon; length of the colon; mouse body weight, immunofluorescence and gene expression analyses; rectal bleeding and histological scoring. First, NIRF imaging of the abdominal area is performed after 3 and 6 injections of DEX-SPNs, corresponding to day 7 and 14 after starting the DSS administration. Note that high Cy5-SPN accumulation (i.e.: high NIRF signal intensity) correlates with high tissue permeability and disease severity. On the contrary, low Cy5-SPN accumulation (i.e.: low NIRF signal intensity) correlates with low tissue permeability. Since an effective therapy should reduce tissue permeability, a lower Cy5-SPN accumulations would be associated with a successful therapeutic intervention. **Figure 4A** presents live animal NIRF images taken at day 8 after starting DSS administration. The highest signal is observed for Empty SPNs, followed by the Free DEX, DEX-SPNs and the normal animal (**Figure 4A and 4B**). Specifically, as compared to the normal mouse, the NIRF signal intensity is enhanced by 30 and 15-fold for the Empty SPNs and Free DEX and by only 5-fold for the DEX-SPNs (**Figure 4B)**. NIRF imaging on the harvested colons confirms the same trend observed on living animals (**Figure 4C**). Also, the length of the colon treated with DEX-SPNs is statistically similar to the healthy control (3.01 ± 0.08 vs 3.23 ± 0.13 cm), whereas the colon of the mice treated with Free DEX is significantly shorter (2.60 ± 0.14 cm) and much shorter in the case of Empty SPNs (2.35 ± 0.06 cm) (**Figure 4C)**. **Figure S3.A** presents live animal NIRF images taken at 24h post the injection 6 of DEX-SPNs (day 14 after starting the DSS administration). The highest signal is again observed for Empty SPNs, followed by DEX-SPNs and the normal animal (**Figure S3.A-B**). Specifically, as compared to the normal mouse, the NIRF signal intensity is enhanced by 20-fold for the Empty SPNs, whereas no appreciable difference is observed between DEX-SPNs treated mice and normal animals. This is also evident in the NIRF imaging of the harvested colons (**Figure S3.C**). The length of the colon treated with DEX-SPNs is similar to the healthy control (about 3.0 cm), whereas the colon of the mice treated with Empty SPNs is significantly shorter (2.5 cm). Importantly, none of the mice treated with intravenously injected Free DEX survived longer than 13 days, whereas 90% of the DEX-SPNs treated mice and 50% of the Empty SPN administered mice survived over 15 days (**Figure S3.D**). The actual colon lengths are presented in **Figure S3.E** for all experimental groups. It is evident in **Figure S4.A-B**¸ the extensive damage induced in the colon of the Free DEX and Empty SPN administered mice as compared to the normal and DEX-SPNs administered mice. In the former case, the intestinal mucosa shows profound signs of alteration and laceration which are not visible in the control and DEX-SPNs treated animals. The worse conditions are associated with the intravenously administered Free DEX for two reasons: DEX low aqueous solubility limits its bioavailability and biodistribution, as compared to the nanoparticle formulation; treatments with glucocorticoids, such as DEX, are associated with increased water drinking.[30] This would explain the rapid deterioration of the conditions for the Free DEX treated mice that tend to drink more over the first 4 days as compared to normal mice (**Figure S4.C-D**).

During the whole treatment, the body weight of each mouse is also monitored showing that the lowest weight drop and faster recovery are associated with the DEX-SPNs treated mice (**Figure 4D**). Precisely, these mice present a body weight loss of 20% within the first 6 days of DSS administration and reach the body weight of control animals within the following 9 days; whereas mice treated with free DEX show a 30% drop in body weight within the first 8 days and cannot recover the body weight of control animals within the period of observation. Note that Empty SPNs return similar data as for Free DEX treated mice. This should be again related to the treatment with glucocorticoids and the increased water drinking.[30] Therefore, the minimal difference observed in weight reduction between Free DEX and Empty SPN groups as well as the higher body weight drops recorded, as compared to **Figure 3D**, should be ascribed to the higher amounts of water intakes associated with DEX treated mice (see **Figure S4.C-D**). This data supports the notion that SPNs accumulate within the diseased tissue and successfully release DEX modulating the inflammatory state and adverse effects more efficiently than free DEX.

Then, the expression of the inflammatory cytokines TNF-α, IL-1β, and IL-6 is analyzed by immunofluorescence staining of colon sections, as documented in **Figure 5** and **Figure S5** and **S6**.

Representative slides for the expression of TNF-α within the colon tissue in the four treatment groups are shown in **Figure 5**. From top to bottom, this figure shows staining for cell nuclei (blue: DAPI), for SPNs (red: Cy5), for macrophages (yellow: CD68), for TNF-α (green: anti-TNF-α), and merging of all fluorescent channels. It is evident a progressive decrease in TNF-α expression moving from the case of Empty SPNs, to Free DEX and DEX-SPNs. This trend nicely correlates with the macrophage density (third line) and SPN accumulation (second line) within the colon tissue. Note that the density of macrophages and SPN accumulation within the colon of mice treated with DEX-SPNs is very minimal and comparable with the control experiment demonstrating the efficacy of the nano-based intervention. Similar data are available for the other two cytokines, IL-1β and IL-6, in the **Figure S5** and **S6**. To confirm this data, real time PCR and western blot analyses are also conducted on the harvested colon tissues **(Figure 6A-6D)**. It is shown that DEX-SPNs treatment more efficiently reduce the expression of all three inflammatory cytokines as compared to Empty SPNs and Free DEX (TNF-α: **Figure 6A**; IL-1β: **Figure 6B**; and IL-6: **Figure 6C**). Similar data are presented from extracted colon proteins in **Figure 6D**. Note that no statistically significant difference is observed for the expression of TNF-α, IL-1β and IL-6 in comparing mice treated with DSS (IBD group) and mice treated with DSS and injected with Empty SPNs (Empty SPNs group). This demonstrates that Empty SPNs have no influence on the disease state.

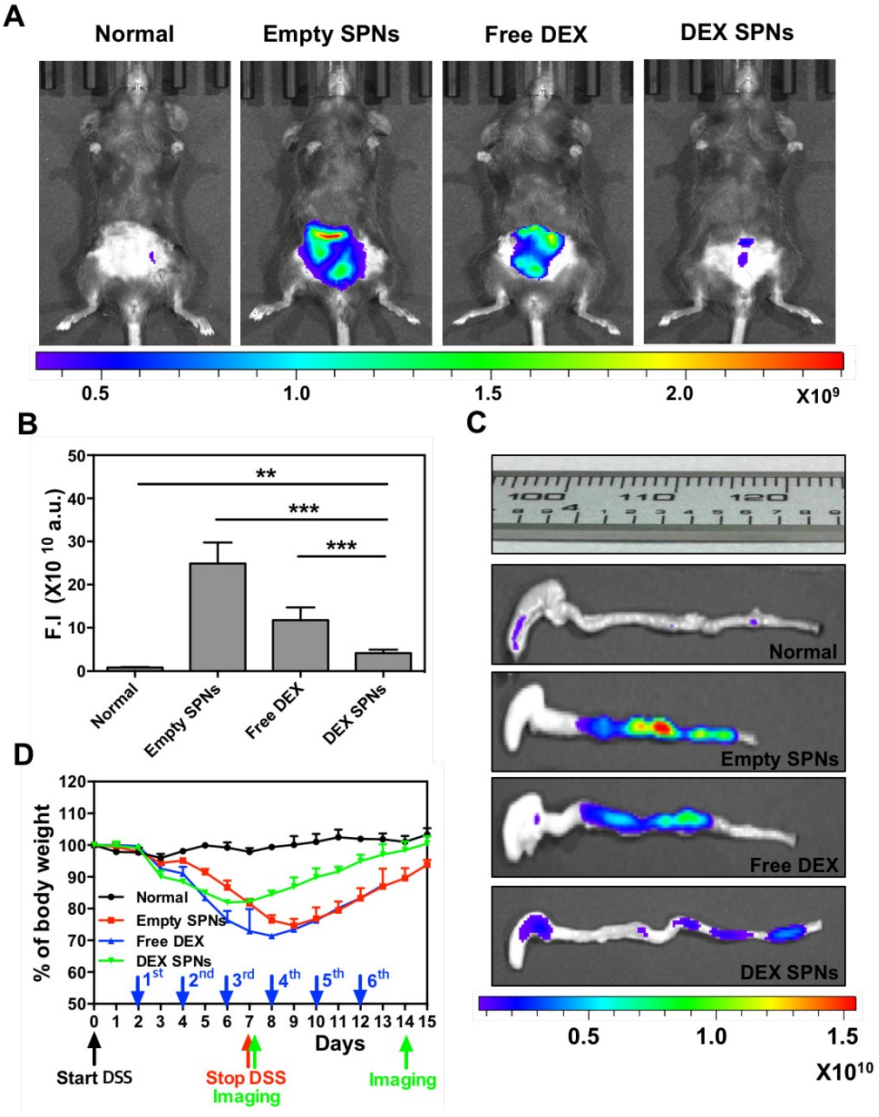

Figure 4. Three times treatment therapeutic efficacy and NIRF imaging with SPNs in DSS-induced mouse models of colitis. A. Representative near-infrared fluorescent (NIRF) *in vivo* image of Cy5-SPNs accumulating within the abdominal area of mice administered with DSS for 7 consecutive days, after three consecutive 3 times treatment sessions with Empty SPNs, Free DEX and DEX-SPNs. **B.** Normalized NIRF signal intensities from the *in vivo* images. **C.** *Ex vivo* colon NIRF imaging and length. **D.** Body weight variation over time of mice administered with DSS. Results are presented as mean ± SD (n=5/group). * $P < 0.05$; ** $P < 0.01$; *** $P < 0.001$

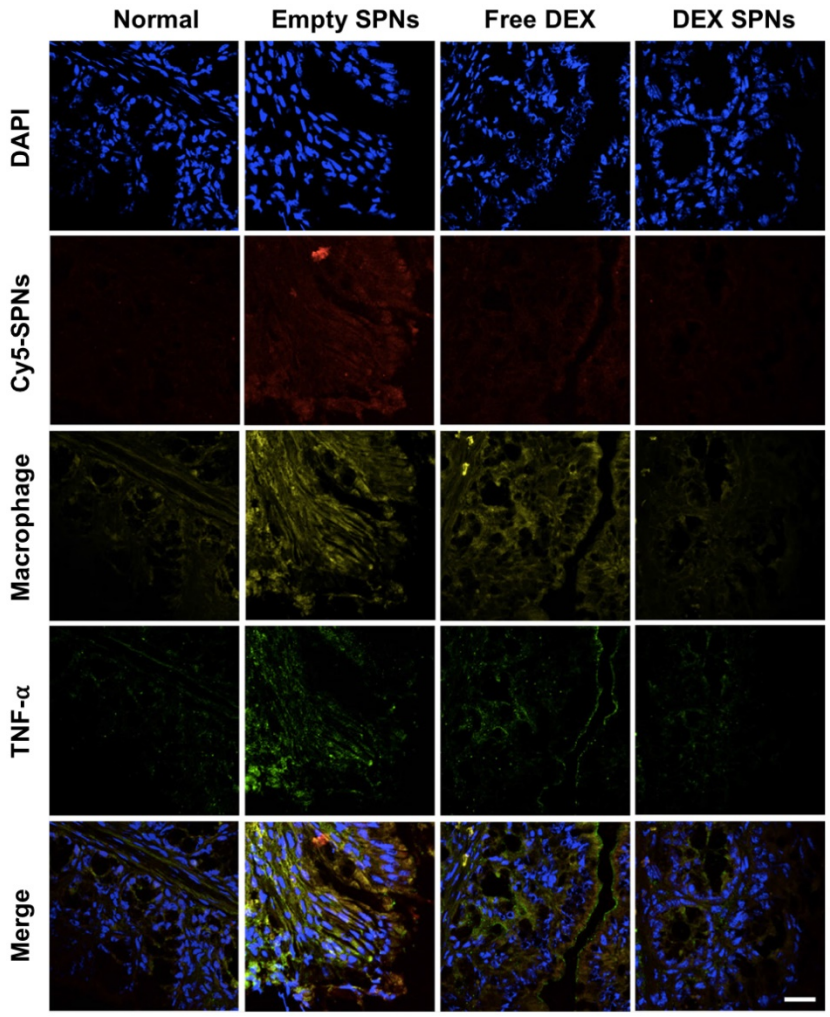

Figure 5. Immunofluorescence staining of intestinal tissues from DSS-induced mouse models of colitis. Histological analysis of TNF-α protein expression after three consecutive treatment sessions with Empty SPNs, Free DEX and DEX-SPNs. (Blue: DAPI, Red: Cy5-SPNs, Yellow: Macrophage, Green: TNF-α)

Finally, in order to further confirm the efficacy of the DEX-SPN treatment over free DEX, a rectal bleeding analysis and a histological scoring of hematoxylin/eosin-stained colon sections have been performed.[29] Data are reported in **Figure 6E**, for the rectal bleeding analysis, and **Figure 6F** for the histological scoring. In both cases, DEX-SPN treatment returns better scores as compared to the other experimental groups thus confirming its superior efficacy in alleviating intestinal inflammation.

It is here important to recall that often IBD tends to manifest as a systemic disease where macrophages in other biological districts, such as the liver, are also stimulated.[31, 32] This trend is confirmed in the DSS-induced colitis model used in this manuscript. The **Figure S2.A** shows ex vivo NIRF imaging of Cy5-SPNs which have accumulated in different organs upon systemic injection. Specifically, NIRF images are presented, from left to right, for the liver (L), lungs (P), kidneys (K), spleen (S), heart (H) and intestine (I). Interestingly, the intensity of the NIRF signal for the liver grows significantly with the severity of the disease (5, 7 and 10 days of DSS administration) following the intensity detected for the intestines. Since the liver hosts a multitude of tissue specific macrophages (Kupffer cells), the increased NIRF signal should be ascribed to local tissue inflammation and the increased ability of Kupffer cells to uptake circulating SPNs. Indeed, this is confirmed by immunofluorescence staining of liver tissue sections (**Figure S7 – S9**). The fluorescent signals for Cy5-SPNs (second line), macrophages (third line) and TNF-α (fourth line) (**Figure S7**) are elevated in the mice treated with Empty SPNs and Free DEX, whereas no significant difference is observed when comparing normal (no DSS administration) and DEX-SPNs treated mice. Same data are presented in **Figure S8-S9** for IL-1β and IL-6. Furthermore, significant inflammation in the liver

and, at a lower extent, in the kidneys and lungs is also demonstrated via NIRF imaging, upon injection of the inflammation sensitive dye Prosense, as documented in **Figure.S10**. This is a notable result in that it demonstrates that DEX-SPNs not only are capable of modulating inflammation locally, in the intestine, but also systemically. Furthermore, the higher therapeutic efficacy of DEX-SPNs over Free DEX is confirmed and should most likely be ascribed to the improved biodistribution of DEX encapsulated within SPNs over its freely administered form, both as DEX acetate and DEX phosphate (**Figure.S11**).

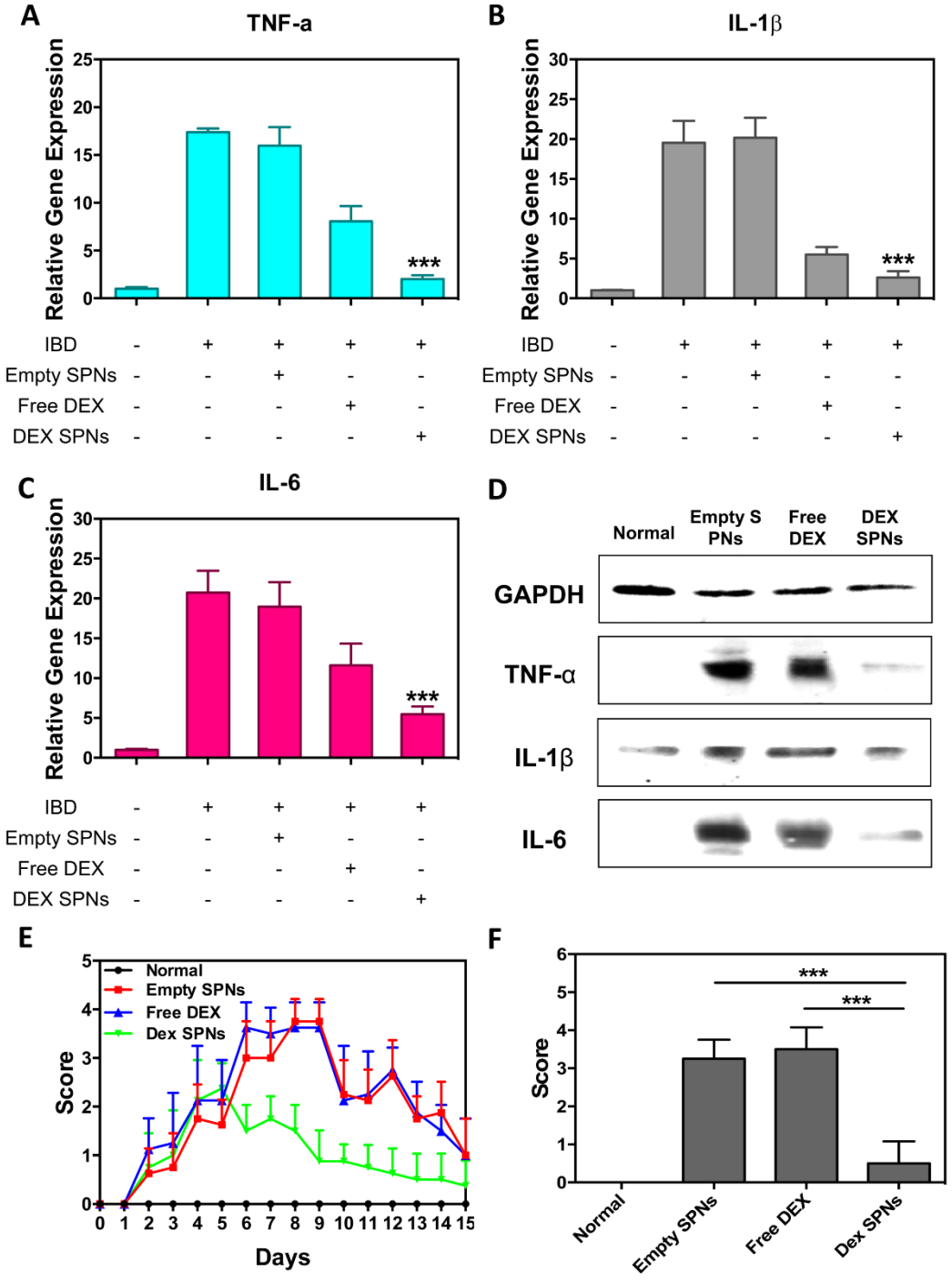

Figure 6. Scoring of intestinal bleeding/ Histological change and *ex vivo* gene/ protein expression. A. TNF-α, **B.** IL-1β, **C.** IL-6, after three consecutive treatment sessions with Normal, IBD control, Empty SPNs, Free DEX and DEX-SPNs. Results are presented as mean ± SD (n=3/group). *** indicates $P < 0.001$, DEX SPNs vs IBD control, Empty SPNs, Free DEX, or Normal. **D.** Protein levels of TNF-α, IL-1β, and IL-6 within the intestinal tissue in DSS-induced mouse models of colitis. TNF-α (17 kDa), IL-1β (17 kDa), and IL-6 (24 kDa) bands are shown. GAPDH is used as the internal control (40 kDa). **E.** Intestinal bleeding score. **F.** histology score for the four experimental groups (normal, Empty SPNs, Free DEX and DEX SPNs). Results are presented as mean ± SD (n=3/group). *** indicates $P < 0.001$.

Conclusions

Building on the successes of nanomedicines in treating and imaging solid cancers and atherosclerotic plaques, dexamethasone loaded spherical polymeric nanoconstructs (DEX-SPNs) are here demonstrated for the anti-inflammatory treatment and near infrared imaging of DSS-induced colitis. The higher permeability of the intestinal inflamed tissue facilitates the stable accumulation of systemically injected SPNs, as demonstrated via in vivo and ex vivo NIRF imaging; the rapid internalization of SPNs into cells of the immune system favors the effective intracellular release of dexamethasone and the consequent modulation of the inflammatory response, as documented by the multi-fold decrease in the expression of pro-inflammatory genes (TNF-α, IL-1β, IL-6). In preclinical models of DSS-induced colitis, DEX-SPNs significantly reduce mouse weight loss and facilitates recovery as compared to free DEX. Importantly, the intravenously injected DEX-SPNs are shown to exert their potent anti-inflammatory effect locally, within the inflamed colon, and systemically.

In conclusion, it is important to recall that nanoconstructs can be used for the co-delivery of multiple therapeutic agents, potentially teaming dexamethasone with other anti-inflammatory molecules or with specifically targeted RNAs.[23] [24] Also, nanoconstructs can be employed for assessing non-invasively the efficacy of the medical intervention via imaging. This should stimulate additional efforts in the development and optimization of nanoconstructs against inflammatory bowel disease and chronic inflammation.

Supplementary Material

Supplementary figures and tables.
http://www.thno.org/v07p3653s1.pdf

Acknowledgements

The authors acknowledge the support from the Electron Microscopy Laboratory and Animal Facility at the Italian Institute of Technology in Genoa.

Funding

This project was partially supported by the European Research Council, under the European Union's Seventh Framework Programme (FP7/2007-2013)/ERC grant agreement no. 616695; AIRC (Italian Association for Cancer Research) under the individual investigator grant no. 17664; the Italian Institute of Technology.

Contributors

The study was designed by AL and PD. AL synthesized and characterized the spherical polymeric nanoconstructs, performed in vitro and in vivo experiments. CDM helped with the animal experiments and performed the flow cytometry analysis. MF synthesized lipid-Cy5 and Cy5-SPNs for NIRF imaging. RM performed EM analyses. HYY helped with the animal experiments. AL, KK, ICK and PD wrote the manuscript. PD coordinated the project. Results were analyzed and discussed by all authors.

Competing Interests

The authors have declared that no competing interest exists.

References

1. Podolsky DK. Inflammatory bowel disease. The New England journal of medicine. 2002; 347: 417-29.
2. Abraham C, Cho JH. Inflammatory bowel disease. The New England journal of medicine. 2009; 361: 2066-78.
3. Xavier RJ, Podolsky DK. Unravelling the pathogenesis of inflammatory bowel disease. Nature. 2007; 448: 427-34.
4. Johansson ME, Gustafsson JK, Holmen-Larsson J, Jabbar KS, Xia L, Xu H, et al. Bacteria penetrate the normally impenetrable inner colon mucus layer in both murine colitis models and patients with ulcerative colitis. Gut. 2014; 63: 281-91.
5. Steinbach EC, Plevy SE. The role of macrophages and dendritic cells in the initiation of inflammation in IBD. Inflammatory bowel diseases. 2014; 20: 166-75.
6. Chin AC, Parkos CA. Neutrophil transepithelial migration and epithelial barrier function in IBD: potential targets for inhibiting neutrophil trafficking. Annals of the New York Academy of Sciences. 2006; 1072: 276-87.
7. Brazil JC, Parkos CA. Pathobiology of neutrophil-epithelial interactions. Immunological reviews. 2016; 273: 94-111.
8. Koelink PJ, Overbeek SA, Braber S, Morgan ME, Henricks PA, Abdul Roda M, et al. Collagen degradation and neutrophilic infiltration: a vicious circle in inflammatory bowel disease. Gut. 2014; 63: 578-87.
9. Irvine EJ, Marshall JK. Increased intestinal permeability precedes the onset of Crohn's disease in a subject with familial risk. Gastroenterology. 2000; 119: 1740-4.
10. Soderholm JD, Olaison G, Lindberg E, Hannestad U, Vindels A, Tysk C, et al. Different intestinal permeability patterns in relatives and spouses of patients with Crohn's disease: an inherited defect in mucosal defence? Gut. 1999; 44: 96-100.
11. Teshima CW, Dieleman LA, Meddings JB. Abnormal intestinal permeability in Crohn's disease pathogenesis. Annals of the New York Academy of Sciences. 2012; 1258: 159-65.
12. Gibson PR. Increased gut permeability in Crohn's disease: is TNF the link? Gut. 2004; 53: 1724-5.
13. Mowat C, Cole A, Windsor A, Ahmad T, Arnott I, Driscoll R, et al. Guidelines for the management of inflammatory bowel disease in adults. Gut. 2011; 60: 571-607.
14. Lautenschlager C, Schmidt C, Fischer D, Stallmach A. Drug delivery strategies in the therapy of inflammatory bowel disease. Adv Drug Deliv Rev. 2014; 71: 58-76.
15. Higgins PD, Skup M, Mulani PM, Lin J, Chao J. Increased risk of venous thromboembolic events with corticosteroid vs biologic therapy for inflammatory bowel disease. Clinical gastroenterology and hepatology : the official clinical practice journal of the American Gastroenterological Association. 2015; 13: 316-21.
16. Wang AS, Armstrong EJ, Armstrong AW. Corticosteroids and wound healing: clinical considerations in the perioperative period. American journal of surgery. 2013; 206: 410-7.
17. Peer D, Karp JM, Hong S, Farokhzad OC, Margalit R, Langer R. Nanocarriers as an emerging platform for cancer therapy. Nat Nanotechnol. 2007; 2: 751-60.
18. Min Y, Caster JM, Eblan MJ, Wang AZ. Clinical Translation of Nanomedicine. Chem Rev. 2015; 115: 11147-90.
19. Lee A, Di Mascolo D, Francardi M, Piccardi F, Bandiera T, Decuzzi P. Spherical polymeric nanoconstructs for combined chemotherapeutic and anti-inflammatory therapies. Nanomedicine-Uk. 2016.
20. Stigliano C, Key J, Ramirez M, Aryal S, Decuzzi P. Radiolabeled Polymeric Nanoconstructs Loaded with Docetaxel and Curcumin for Cancer Combinatorial Therapy and Nuclear Imaging. Advanced Functional Materials. 2015; 25: 3371-9.
21. Mura S, Nicolas J, Couvreur P. Stimuli-responsive nanocarriers for drug delivery. Nat Mater. 2013; 12: 991-1003.
22. Key J, Palange AL, Gentile F, Aryal S, Stigliano C, Di Mascolo D, et al. Soft Discoidal Polymeric Nanoconstructs Resist Macrophage Uptake and Enhance Vascular Targeting in Tumors. ACS nano. 2015; 9: 11628-41.

23. Peer D, Park EJ, Morishita Y, Carman CV, Shimaoka M. Systemic leukocyte-directed siRNA delivery revealing cyclin D1 as an anti-inflammatory target. Science. 2008; 319: 627-30.
24. Laroui H, Theiss AL, Yan Y, Dalmasso G, Nguyen HT, Sitaraman SV, et al. Functional TNFalpha gene silencing mediated by polyethyleneimine/TNFalpha siRNA nanocomplexes in inflamed colon. Biomaterials. 2011; 32: 1218-28.
25. Maeda H. Macromolecular therapeutics in cancer treatment: the EPR effect and beyond. Journal of controlled release : official journal of the Controlled Release Society. 2012; 164: 138-44.
26. Kamaly N, Fredman G, Subramanian M, Gadde S, Pesic A, Cheung L, et al. Development and in vivo efficacy of targeted polymeric inflammation-resolving nanoparticles. Proceedings of the National Academy of Sciences of the United States of America. 2013; 110: 6506-11.
27. Kiesler P, Fuss IJ, Strober W. Experimental Models of Inflammatory Bowel Diseases. Cellular and molecular gastroenterology and hepatology. 2015; 1: 154-70.
28. Lee A, Di Mascolo D, Francardi M, Piccardi F, Bandiera T, Decuzzi P. Spherical polymeric nanoconstructs for combined chemotherapeutic and anti-inflammatory therapies. Nanomedicine. 2016; 12: 2139-47.
29. Wirtz S, Neufert C, Weigmann B, Neurath MF. Chemically induced mouse models of intestinal inflammation. Nat Protoc. 2007; 2: 541-6.
30. Thunhorst RL, Beltz TG, Johnson AK. Glucocorticoids increase salt appetite by promoting water and sodium excretion. American journal of physiology Regulatory, integrative and comparative physiology. 2007; 293: R1444-51.
31. Funderburg NT, Stubblefield Park SR, Sung HC, Hardy G, Clagett B, Ignatz-Hoover J, et al. Circulating CD4(+) and CD8(+) T cells are activated in inflammatory bowel disease and are associated with plasma markers of inflammation. Immunology. 2013; 140: 87-97.
32. Uko V, Thangada S, Radhakrishnan K. Liver disorders in inflammatory bowel disease. Gastroenterology research and practice. 2012; 2012: 642923.